

Observed rotational enhancement of nonlinear optical vortices

D. Rozas and G. A. Swartzlander, Jr.

Department of Physics, Worcester Polytechnic Institute, Worcester, Massachusetts 01609-2280

Received September 23, 1999

The propagation dynamics of an optical vortex pair is experimentally confirmed to experience enhanced rotation in a self-defocusing medium. We measured this effect to be 3.5 times larger than in linear media. The enhancement is attributed to nonlinear refraction within the dark vortex cores, permitting the vortices to propagate as vortex filaments. © 2000 Optical Society of America

OCIS codes: 190.0190, 190.4420, 190.4870, 350.5030, 350.5500, 090.1760.

Optical vortices (OV's) are ubiquitous in coherent optical fields.¹⁻⁷ They have also been discovered to propagate as solitons in self-defocusing Kerr nonlinear refractive media.^{8,9} Surprisingly, OV's may also develop from an initially smooth beam in weakly nonlinear media.¹⁰⁻¹³ Investigations of beams that contain pointlike vortices or multiple vortices often take advantage of computer-generated holographic techniques.¹⁴⁻¹⁶ Such vortices are characterized by a beam whose phase velocity circulates about a small dark vortex core. The phase is azimuthally harmonic, and thus the intensity vanishes at the center of the core owing to destructive interference.

When two or more vortices are entangled in the same beam, an effective interaction is established by means of phase gradients. For example, two identical point vortices separated by a distance d_v will rotate about their midpoint at a rate proportional to $1/d_v^2$. A similar effect occurs between vortices in continuous media (e.g., two nearby hurricanes) through the flow fields.¹⁷ This optical effect, however, has been observed only when the OV cores do not overlap.⁶ In most cases, amplitude gradients, which also affect the propagation dynamics of vortices, essentially cancel the effects of the phase gradient when the cores overlap.¹⁸ Owing to the diffraction of point vortices in linear optics, the cores eventually overlap, and rotation slows. In a self-defocusing medium, however, one may offset diffraction with nonlinear refraction, and thus the OV's can be prevented from overlapping. Numerical calculations¹⁸ predict enhanced vortex rotation angles in nonlinear media that exceed the linear optics limit of 90° (the Gouy phase¹⁹). In this Letter we describe what we believe is the first experimental verification of this enhancement.

The envelope function that describes N OV's entangled in a background beam, E_{BG} , may be written in multipolar coordinates:

$$E(r, \theta, z) = E_{BG}(r, z) \prod_{j=1}^N A_j(r_j, z) \exp(im_j \theta_j), \quad (1)$$

where A_j is a complex amplitude that describes the vortex core, m_j is the topological charge of the j th vortex, and (r_j, θ_j) are circular coordinates defined with

respect to an origin at each vortex core. In practice, the initial background field is often a Gaussian distribution: $E_{BG}(r, 0) = E_0 \exp(-r^2/w_0^2)$, where w_0 is the beam waist and E_0^2 is a characteristic intensity. In this Letter we are concerned with two identical vortices ($N = 2, m_1 = m_2 = 1$) placed symmetrically about (and near) the optical axis, as shown in Fig. 1. The vortices in Eq. (1) may form OV solitons in a self-defocusing Kerr material that has a nonlinear coefficient, $n_2 < 0$.^{8,9} Ideally the core size converges toward the soliton size, $w_v \approx 1.270k^{-1}(n_0/\Delta n)^{1/2}$ as the beam propagates, and the amplitude profile near the core reaches a stationary state approximated by

$$A_j(r_j, z) \approx \tanh(r_j/w_j) \exp(i\Delta n k z), \quad (2)$$

where $\Delta n = -n_2 E_0^2$ and n_0 are nonlinear and linear refractive indices, respectively, and k is the wave number. In our experiment, the vortex cores at the input face of the nonlinear cell were made larger (by diffraction) than the soliton size. At low beam power the cores overlap, but as the beam power is increased the cores contract. As the core diameters become smaller than the vortex separation distance ($2w_v < d_v$), we expect to observe the predicted rotational enhancement. A contraindication of this enhancement, which may be attributed to the use of a small background beam ($w_0 \sim d_v$),¹⁸ was observed by Luther-Davies *et al.*²⁰

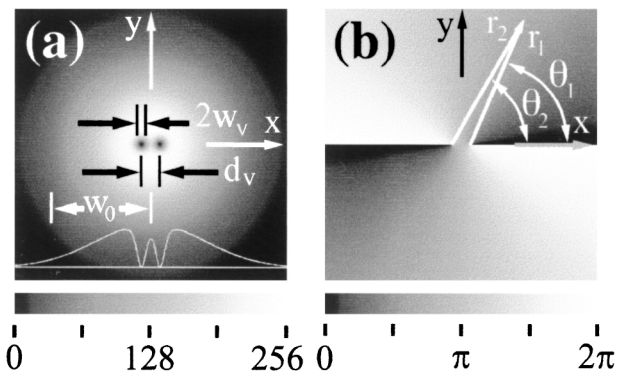


Fig. 1. (a) Intensity and (b) phase profiles of two identical small-core vortices near the center of a Gaussian beam in the initial transverse plane ($z = 0$).

To achieve the enhancement, we produced a computer-generated hologram consisting of two closely spaced vortices: $d_V \ll w_0$. Two different computer-generated holograms were made that had different values of d_V . They were recorded onto DuPont photopolymer film (HRF-150X001-38) at a fringe spacing of roughly $1 \mu\text{m}$ to achieve a high-efficiency, high-damage-threshold phase hologram. The core size in the plane of the hologram was measured to be $w_V = 30 \pm 5 \mu\text{m}$ for vortices separated by $d_V = 135 \pm 4 \mu\text{m}$ and $w_V = 45 \pm 5 \mu\text{m}$ for vortices separated by $d_V = 84 \pm 4 \mu\text{m}$.

A schematic of the optical system is shown in Fig. 2. An argon-ion laser beam ($\lambda = 0.514 \mu\text{m}$, $P \approx 6 \text{ W}$, $w_0 = 1 \text{ mm}$) was directed through beam splitter BS₁ and a hologram and into a vertically aligned glass cell of length $l_C = 290 \text{ mm}$ that contained a self-defocusing material, slightly dyed methanol ($n_0 = 1.33$) with an absorption coefficient $\alpha = 2.4 \times 10^{-3} \text{ mm}^{-1}$. The distance between the hologram and the input face of the cell was $l_{\text{air}} = 230 \text{ mm} > z_v$, where $z_v = (1/2)d_v^2$ is a characteristic diffraction length for the vortex pair. The net optical path between the hologram and the output face of the cell was $l_{\text{net}} = l_{\text{air}} + n_0 l_C = 616 \text{ mm}$. The output face of the cell was imaged with lens L₁ onto a CCD camera. The beam splitters in Fig. 2 were arranged to form a Mach-Zehnder interferometer, permitting easy identification of the vortex centers (which occur at forks in the fringe pattern). Images were recorded after an illumination period of roughly 3 s to allow the thermal nonlinear system to reach a quasi-steady state.

The recorded output intensity profiles are shown in Fig. 3 for $d_V = 84 \pm 4 \mu\text{m}$ at four values of the beam power (measured at the input face). From interferograms of such images (not shown) we determined the angular displacement ϕ_V with respect to the initial position (-11.5° from the x axis) in the plane of the hologram. In the low-power regime, shown in Fig. 3(a), linear diffraction allows the vortices not only to rotate by $\phi_V = 29^\circ$ but also to completely overlap each other. As the laser power is increased, the vortex cores contract and become resolvable, as shown in Figs. 3(b)–3(d), owing to nonlinear refraction. As expected, the angular position of the vortices is found to increase with increasing power. Surprisingly, we also found that the cores become elongated at higher powers, as if the vortex axes themselves were tilted away from the optical axis. An analogous instability owing to torsion from perturbations and self-interactions is observed in fluid dynamics.²¹ Perturbations from nonlocal heating effects may be the source of this instability in our experiments. We also point out that, as the vortex cores contract, the area of the beam expands owing to self-defocusing, and an optical shock front is established at the perimeter of the beam, as seen in Fig. 4. The vortex cores also radiate during contraction, as evidenced by the high-intensity ring surrounding the pair of vortices in Fig. 4.

The power-dependent angular displacement of the vortices is plotted in Fig. 5(a) for both holograms. In both cases the value of ϕ_V initially increases as the power increases and then tends to saturate (at

$P_0 \sim 0.8 \text{ W}$) once the vortex cores cease to overlap. Surprisingly, for $d_V = 135 \mu\text{m}$ the saturation gives way to a second regime of rotational enhancement for $P_0 > 1.5 \text{ W}$. In this case the net rotation angle reaches $\phi_V = 106 \pm 3^\circ$, exceeding the linear optics limit of 90° . Compared with the linear angular displacement of 30° (with respect to the initial orientation along the x axis), this constitutes an enhancement of 3.5 times. We note that even larger enhancements were achieved in the transient regime (e.g., within 1/30 s) before heat diffused across the vortex cores.

The radiated ring surrounding the vortices in Fig. 4 may contribute to this enhancement. An amplitude gradient in the vicinity of a vortex core, $\nabla_\perp(E/A_i)$, effectively pushes the vortex in the direction perpendicular to the gradient.¹⁸ In our experiment the vortices

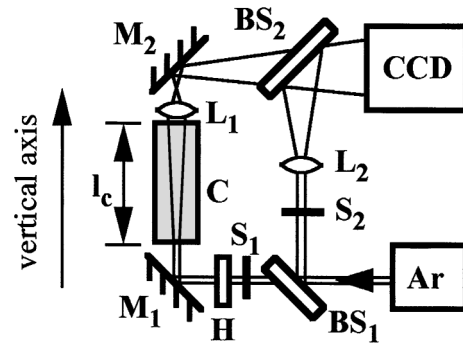


Fig. 2. Experimental setup: Ar, argon-ion laser ($\lambda = 514 \text{ nm}$); H, holographic recording of two identical small-core vortices; M₁, M₂, mirrors, C, vertical glass cell of length $l_C = 29 \text{ cm}$ filled with weakly absorbing liquid (dyed methanol); L₁, L₂, lenses of focal distance $d = 50 \text{ mm}$; CCD, CCD camera and frame grabber; S₁, S₂, shutters.

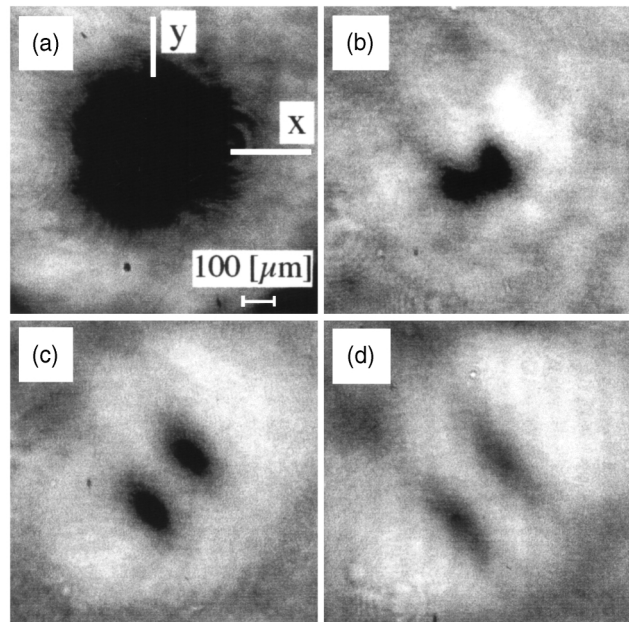


Fig. 3. Output intensity profiles for incident powers of $P_0 =$ (a) 0.01, (b) 0.4, (c) 1.9, and (d) 2.5 W. In the plane of the hologram (not shown), $d_V = 84 \pm 4 \mu\text{m}$ and the initial vortex alignment is -11.5° below the x axis.

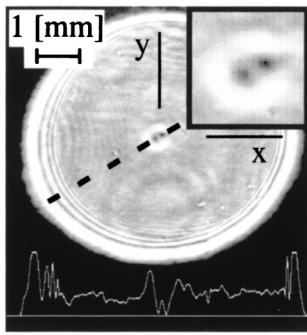


Fig. 4. Transverse intensity profile for the nonlinear case, $P_0 = 0.54$ W, showing optical blooming at the edge of the beam as well as a radiation ring surrounding the vortices. The intensity along the dashed line is plotted at the bottom.

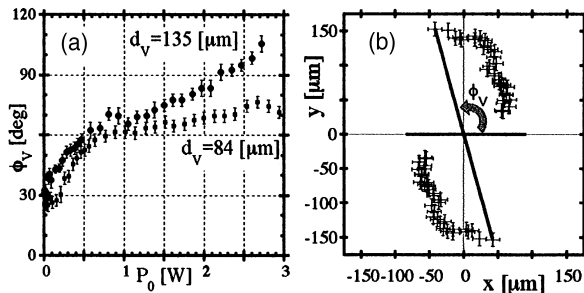


Fig. 5. (a) Plots of measured values of angular displacement ϕ_V versus incident power P_0 for initial vortex separations of $d_V = 84 \pm 4 \mu\text{m}$ and $d_V = 135 \pm 4 \mu\text{m}$. (b) Vortex trajectories for $d_V = 135 \pm 4 \mu\text{m}$ and the initial vortex alignment along the x axis.

clearly reside along the inside rim of the radiation ring (see Fig. 3). Hence both the phase and the amplitude of the beam may contribute to the rotation of the vortex pair under high-power illumination. What is somewhat surprising to us is that this additional rotational enhancement occurs even though the distance between the vortex cores increases owing to beam expansion. The transverse position of the vortices is shown in Fig. 5(b) at different values of the beam power. The radial position of the cores increases by a factor of 2.1 at $P = 2.6$ W for $d_V = 135 \mu\text{m}$. Thus the component of the rotational rate caused by vortex phase gradients is expected to decrease by a factor of 1/4. Therefore we believe that the observed anomalous rotational enhancement is caused by the large amplitude gradient of the radiated ring.

In summary, we have observed an enhancement of the fluidlike rotation of optical vortices owing to a contraction of the vortex cores in a nonlinear refractive medium. As the cores contract, a ring of light is radiated from the cores. The vortex cores were observed

to exhibit a second regime of rotational enhancement, which we attribute to the amplitude gradient of this ring. Owing to these nonlinear effects we have observed, for the first time to our knowledge, vortex rotation angles that exceed the 90° Gouy phase limit.

We gratefully acknowledge discussion with C. T. Law, University of Wisconsin, Milwaukee. This research was supported by the Research Corporation, the National Science Foundation, Spectra-Physics Lasers, Inc., and the Newport Corporation. G. A. Swartzlander's e-mail address is grovers@wpi.edu.

References

1. G. Goubau and F. Schwing, IRE Trans. Antennas Propag. **9**, 248 (1961).
2. W. H. Carter, Opt. Acta **21**, 871 (1974).
3. J. F. Nye and M. V. Berry, Proc. R. Soc. London Ser. A **336**, 165 (1974).
4. N. B. Baranova, B. Ya. Zel'dovich, A. V. Mamaev, N. F. Pilipetskii, and V. V. Shkunov, Pis'ma Zh. Eks. Teor. Fiz. **33**, 206 (1981) [JETP Lett. **33**, 195 (1981)].
5. G. Indebetow, J. Mod. Opt. **40**, 73 (1993).
6. D. Rozas, Z. S. Sacks, and G. A. Swartzlander, Jr., Phys. Rev. Lett. **79**, 3399 (1997).
7. G. A. Swartzlander, Jr., in *Optical Vortices*, M. Vasnetsov and K. Staliunas, eds., Vol. 228 of Horizons in World Physics (Nova, Commack, N.Y., 1999), pp. 107–124.
8. G. A. Swartzlander, Jr., and C. T. Law, Phys. Rev. Lett. **69**, 2503 (1992).
9. A. W. Snyder, L. Poladian, and D. J. Mitchell, Opt. Lett. **17**, 789 (1992).
10. T. Ackemann, E. Kriege, and W. Lange, Opt. Commun. **115**, 339 (1995).
11. A. V. Ilyenkov, A. I. Khizhnyak, L. V. Kreminskaya, M. S. Soskin, and M. V. Vasnetsov, Appl. Phys. B **62**, 465 (1996).
12. A. V. Ilyenkov, L. V. Kreminskaya, M. S. Soskin, and M. V. Vasnetsov, J. Nonlin. Opt. Phys. Mater. **6**, 169 (1997).
13. A. M. Deykoon, M. S. Soskin, and G. A. Swartzlander, Jr., Opt. Lett. **24**, 1224 (1999).
14. V. Yu. Bazhenov, M. V. Vasnetsov, and M. S. Soskin, Pis'ma Zh. Eksp. Teor. Fiz. **52**, 1037 (1990) [JETP Lett. **52**, 429 (1990)].
15. N. R. Heckenberg, R. McDuff, C. P. Smith, and A. G. White, Opt. Lett. **17**, 221 (1992).
16. Z. S. Sacks, D. Rozas, and G. A. Swartzlander, Jr., J. Opt. Soc. Am. B **15**, 2226 (1998).
17. A. Sommerfeld, *Mechanics of Deformable Bodies* (Academic, London, 1950), p. 156.
18. D. Rozas, C. T. Law, and G. A. Swartzlander, Jr., J. Opt. Soc. Am. B **14**, 3054 (1997).
19. L. G. Gouy, Ann. Chim. Phys. Ser. 6 **24**, 145 (1891).
20. B. Luther-Davies, R. Powles, and V. Tikhonenko, Opt. Lett. **19**, 1816 (1994).
21. R. Betchov, J. Fluid Mech. Part 3, **22**, 471 (1965).